Locally defined seasonal rainfall characteristics within the Horn of Africa drylands from rain gauge observations

Katherine Cocking[a], Michael Bliss Singer[a,b,c], David MacLeod[a], Mark O. Cuthbert[a,c], Rafael Rosolem[d], Flavian Muthusi[e], Paolo Paron[e], Joyce Kimutai[f], Phillip Omondi[g], Ahmed Mohamed Hassan[h], Asaminew Teshome[i], Katerina Michaelides[b,d]

[a] *School of Earth and Environmental Sciences, Cardiff University, Cardiff, CF10 3AT, United Kingdom*

[b] *Earth Research Institute, University of California Santa Barbara, USA*

[c] *Water Research Institute, Cardiff University, Cardiff, CF10 3AX, United Kingdom*

[d] *School of Geographical Sciences, University of Bristol, Bristol, BS8 1SS, United Kingdom*

[e] *Food and Agriculture Organization of the United Nations, Somalia Water and Land Information Management (SWALIM) Project Office, P.O. Box 30470-00100, Nairobi, Kenya*

[f] *Kenya Meteorological Department (KMD), Nairobi 00100 GPO, Kenya*

[g] *IGAD Climate Prediction and Application Centre (ICPAC), P.O. Box 10304-00100, Nairobi, Kenya*

[h] *Somali Ministry of Energy and Water Resources, Bondhere District, Mogadishu, Somalia.*

[i] *Ethiopian Meteorological Institute, P.O.BOX 1090, Addis Ababa, Ethiopia*

Corresponding authors: Katherine Cocking, CockingK@Cardiff.ac.uk

Michael Singer, bliss@eri.ucsb.edu

ABSTRACT

Seasonal rainfall is critical to lives and livelihoods within the Horn of Africa drylands (HAD), but it is highly variable in space and time. The HAD rainfall seasons are typically defined as March-April-May (MAM) and October-November-December (OND). However, these three-month periods are only generalised definitions of seasonality across the HAD, and local experience of rainfall may depart from these substantially. Here, we use daily rain gauge data with a duration of at least 10 years from 69 stations across Kenya, Somalia, and Ethiopia to locally delineate key rainfall seasons. By calculating local seasonal rainfall timings, totals, and extremes we obtain more accurate estimates of the spatial variability in rainfall delivery across the HAD, as well as climatological patterns. Results show high spatial variability in season onset, cessation, and length across the region, indicating that a homogenous classification of rainfall seasons across the HAD (e.g. MAM and OND) is inadequate for representing local rainfall characteristics. Our results show that the 'long rains' season is not significantly longer than 'short rains' season over the period of study. This could be related to the previously documented decline of the 'long rains' rainfall totals over recent decades. Several rainfall metrics also vary spatially between seasons, and the rainfall on the most extreme days can accumulate to double the mean seasonal total. The locally defined rainfall seasons better capture the bulk of the rainfall during the season, giving improved characterisation of rainfall metrics, consistent with the aim of a better understanding of rainfall impacts on local communities.

1. Introduction

Seasonal rainfall in the Horn of Africa Drylands (HAD) is a lifeline for rural communities who rely on water from distinct rainfall seasons for crop growth, livestock rearing, and drinking water (Mati 2005; Palmer et al. 2023). Irregular rainfall and droughts have been identified as the leading source of vulnerability to food insecurity within arid and semi-arid areas (Amwata et al. 2016; Funk et al. 2019; Verdin et al. 2005). Analysis of the spatial variability of rainfall metrics of the HAD emphasise broad regional definitions of rainfall seasons (Cattani et al. 2018; Mtewele et al. 2021; Muthoni et al. 2019; Ongoma and Chen 2017). However, a local view of rainfall is required for achieving a more grounded understanding of seasonal rainfall timings and the magnitude of daily extremes. Characterising rainfall based on local information connects directly with the experiences of agropastoral communities, whose livelihoods are tied to rainfall seasons. Here, we use rainfall gauging data to examine rainfall seasonality, totals, and extremes to overcome challenges associated with satellite rainfall products that have the advantage of a spatially homogenous data coverage, but which tend to underestimate daily rainfall extremes (Dinku et al. 2018; Harrison et al. 2019) particularly when rainfall rates are high (Ageet et al. 2022).

A more localised perspective on rainfall is also becoming increasingly important due to the recent multi-season drought that occurred within the Horn of Africa between 2020-2022 (Funk et al. 2023) and the associated impacts these climate hazards have on people's lives and livelihoods. Within the recent 5-season drought, the 'long rains' of 2022 were the driest on the 73-year record (Way-Henthorne 2022), during which over 23 million people across the HAD (Somalia, Ethiopia, and Kenya) endured high levels of acute food insecurity (OCHA 2023). Similarly, extreme flooding in key rainy seasons can have devastating impacts for rural communities living along major rivers (Matanó et al. 2022). If rainfall seasons were locally defined, it could provide a more accurate estimation of the potential impacts of seasons that deliver too much or too little rainfall through analysis of hydrologically relevant metrics (Adloff et al. 2022; Degefu et al. 2021).

Rainfall in the HAD follows a bimodal rainfall regime, where the rainfall is typically characterized by two rainfall seasons, often referred to as MAM and OND (March-April-May, and October-November-December) (Gamoyo et al. 2015; Lyon 2014), or 'long rains' and 'short rains', respectively. A high proportion of studies on the seasonal rainfall across East Africa refer exclusively to MAM and OND (March-April-May, and October-November-December) for the two main rainfall seasons (Gebrechorkos et al. 2019; Hoell and Funk 2014; Yang et al. 2015). However, there are regional differences in the naming and timing of the rainfall seasons across countries in the HAD region with Somalia, Ethiopia, and Kenya using different local names for rainfall occurring at different times of the year. These regional rainfall timings are summarised in Table 1:

Table 1. Regional rainfall season timings. Somalia timings from (Ogallo et al. 2017), Somaliland region timings from (Abdulkadir 2017), Ethiopia timings from (Abebe 2006; Seleshi and Zanke 2004), Ethiopia Borena zone timings from (Bekele and Abera 2008; Birhanu et al. 2017), and Kenya timings from (Camberlin and Okoola 2003; Hastenrath et al. 2011; Onyango 2014)

Country/region	Season name	Season timing (months)
Somalia	Gu	April - June
Somalia	Deyr	September - November

Somaliland	Gu	April - June
Somaliland	Deyr	August - November
Ethiopia	Belg	February - May
Ethiopia	Kiremt	June - September
Ethiopia	Bega	October - January
Borena, Ethiopia	Genna	Mid March - May
Borena, Ethiopia	Hageya	September – mid November
Kenya	Masika “long rains”	March - May
Kenya	Vuli “short rains”	October - December

Publications from the early 1900s during the British colonial rule of Kenya provide alternative timings for the seasonal rains, including April-June and September-December for the ‘long rains’ and ‘short rains’ respectively (Jones and Evans 1961), and a ‘long rains’ constricted to just April and May (Garnham 1945). The greater interest in Kenya from the English-speaking world throughout modern history, relative to other countries of the HAD, may be the reason why the rainfall seasons of the HAD are still today more generalised to the Kenya-centric definitions of March-May (MAM) and October-December (OND), as well as the terms ‘long rains’ and ‘short rains’. Within Kenya alone, several seasonal rainfall regimes have been identified. However, the ‘long’ and ‘short’ rains occurring in MAM and OND are so well known that this seasonal timing has become known and used as the typical rainfall regime of all of Kenya (Kenworthy 2020). This seasonal delineation is then applied to other areas in East Africa, for example as utilised by the Greater Horn of Africa Climate Outlook Forum (GHACOF) encompassing eleven IGAD Climate Prediction and Applications Centre (ICPAC) member states including Sudan, South Sudan, Djibouti, Eritrea, Tanzania, Uganda, Rwanda, and Burundi in addition to the countries associated with the Horn of Africa; Somalia, Ethiopia, and Kenya. The GHACOF is a forum that discusses seasonal rainfall and its impacts on lives and livelihoods across the greater horn of Africa and issues early warnings to humanitarian organizations and national governments to support interventions to mitigate disaster. Using our results of climatological characteristics of the rainfall seasons, we aim to identify a suitable framework of local characterization of the two main rainfall seasons of the HAD. This could then be applied within the GHACOF process to support more targeted warnings and actions in the region to potential climate hazards in a dryland region where rainfall is not easily predicted (MacLeod et al. 2023).

Existing work states that for Ethiopia, Somalia, and Kenya, the ‘long rains’ – or the season roughly corresponding of the timing of this season - is broadly considered to be the season that brings the most rain (Abdulkadir 2017; Bekele-Biratu et al. 2018; Camberlin and Okoola 2003), and coincides with the main agricultural growing season (Camberlin and Philippon 2002; Liebmann et al. 2017). However, over recent decades, there has been a concerning decline in the ‘long rains’ (Hoell et al. 2017; Lyon and DeWitt 2012), broadly occurring from the 1980s to the late 2000s. This involves a shortening of the season; a later onset in conjunction with an earlier cessation (Wainwright et al. 2019). This observation is of particular interest due to the East Africa Climate Paradox, which describes how models are predicting a wetting trend during this season, whereas observations indicate an opposing drying trend (Lyon and Vigaud 2017). The nomenclature of these rainfall seasons could lead confusion - particularly surrounding season length - due to the fact we may expect the ‘long rains’ to provide less rain than the ‘short rains’ as a result of the ‘long rains’ decline. Therefore, we henceforth shorten the terms ‘long rains’ and ‘short rains’ to LR and SR respectively.

In drylands, mean annual rainfall is low and is often expressed as high intensity, low duration rainfall events. The spatial and temporal variability in rainfall is high, and rainfall delivery is concentrated in seasons which can still contain long dry periods (Nicholson 2011). Since rain gauge networks in this region often have a sparse coverage, global gridded datasets are typically used for modelling and impact analysis. However, satellite rainfall products are not direct measures of rainfall, since they rely on atmospheric measurements of temperature and/or microwave radiation, and they tend to underestimate daily extremes and high rainfall rates (Cavalcante et al. 2020; Dinku et al. 2018; Harrison et al. 2019; Nkunzimana et al. 2020). These high rainfall rates are hazardous to communities as they can generate significant flash flooding through rapid onset surface runoff which can have adverse impacts on people and society via crop loss, infrastructure damage and landslides (Chang’a et al. 2020; Conway et al. 2005). On the other hand, flash floods in ephemeral streams tend to be significant for focused recharge of groundwater aquifers in drylands (Cuthbert et al. 2019; Horton 1933). Given these factors, enhanced understanding of local rainfall is critical both for mitigating the impacts of climatic hazards and improving understanding of groundwater availability, and this may be best accomplished using in situ rain gauge data.

Here, we employ rain gauge data for the HAD within a local seasonal rainfall delineation framework to quantify the timing of onset, cessation, and length of local rainfall seasons and compare these local seasonal timings to those of calendar-defined MAM and OND. There have been previous efforts to delineate the timings of the biannual rainfall seasons of the HAD (Dunning et al. 2016; Omay et al. 2023; Seregina et al. 2019), but most were based on satellite data, not gauge data. These studies tended to focus on interannual variability of seasonal rainfall timings and establishing unimodal and bimodal rainfall regions. Here we did not have enough gauging data to investigate interannual variability. Our focus was on climatology of seasonal rainfall timings, within-season rainfall metrics, and their spatial variability. The method of seasonal onset and cessation to be performed on the gauge data is based on that of Dunning et al. (2016). This same method is used by Schwarzwald et al. (2023). We use the locally delineated rainfall seasons to investigate various seasonal rainfall metrics to generate new climatological understanding of the spatial variability of rainfall timing, totals, and extremes throughout the HAD. It is our broader aim that these locally defined seasonal rainfall metrics can be used to support more informed decision making with respect to seasonal rainfall across the HAD.

2. Methods

a. Gauge data

We use daily rainfall gauge data across 69 stations from Somalia, Ethiopia and Kenya obtained from the Food and Agriculture Organization's Somalia Water And Land Information Management (FAO-SWALIM), the Ethiopian Meteorology Institute (EMI), and the IGAD Climate Prediction and Applications Centre (ICPAC), originally collected by the Kenya Meteorological Department (KMD). Our dataset includes 51 stations in Somalia, and 9 stations each in both Kenya and Ethiopia (Figure 1a). Gauging record lengths vary between stations, where start year ranges from 1990 to 2012, and end year ranges from 2004 to 2022.

To ensure consistency throughout the region and confidence in the data from each station, we set the criteria of having at least 10 (non-continuous) years of daily data at each gauge, with no more than 10% missing data (NaNs). Satisfying these criteria involved removing years from certain stations within the dataset which contained a high proportion of NaNs, therefore, gauge record length is different at each station, and the years involved aren't always continuous. Further information on gauge station data is available in Supplemental Material Table 1.

b. Drylands study region

The first objective with our rainfall data is to establish a contiguous dryland region of analysis. Semi-arid regions are often defined as having an upper threshold of rainfall of 800 mm/y (Mady et al. 2020; Magombeyi et al. 2018; Nyakudya and Stroosnijder 2015; Samwel 2015), although accurate classification of aridity generally also includes characterisation of atmospheric evaporative demand, which can vary on daily to seasonal timescales (Asfaw et al. 2022; Singer et al. 2021). Dry regions such as the HAD are uniformly dominated by evaporative demand, therefore it is a sensible choice to use MAT (mean annual total rainfall) to define aridity, since MAT has a greater influence over aridity here relative to evaporative demand. Based on the histogram of climatological mean annual precipitation (CMAP) at each of our stations, we found a natural break occurs at around 800mm, suggesting stations that receive a CMAP > 800mm are distinct from stations that receive a CMAP < 800mm (Figure 1c). Therefore, we apply a threshold of 800mm CMAP to classify humid vs dryland gauging stations in the HAD (Figure 1a). Note that there are stations with CMAP < 800mm that reside in an area surrounded by CMAP > 800mm stations, which we removed to maintain a contiguous region of analysis. Initially, the dataset included 94 stations, and 25 of these were removed from our dryland regional rainfall analysis.

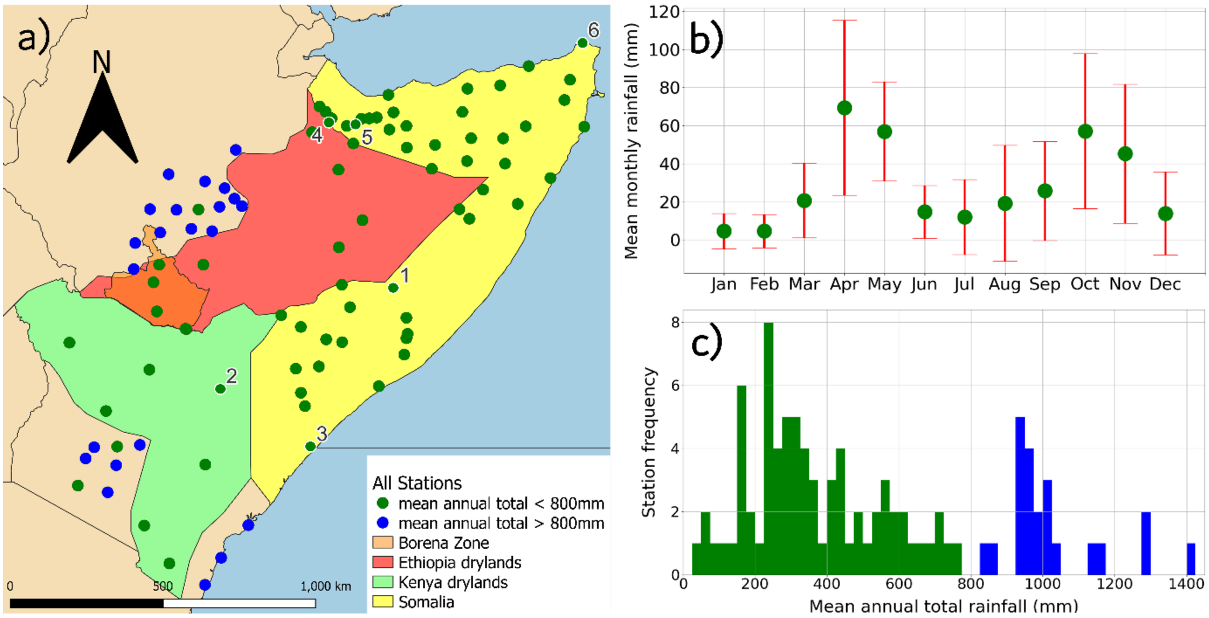

Fig. 1. (a) Map of the Horn of Africa, showing the the drylands study region and the location of the Borena zone within Ethiopia, the rainfall gauge stations in the drylands study region (green), wet stations that were eliminated from analysis (blue), and individually numbered stations including points with white rings which are mentioned subsequently. (b) the seasonal cycle of rainfall shown by mean monthly rainfall totals (green) and standard deviation (red) showing interannual variability, from all stations in the drylands study region. (c) Histogram of climatological mean annual precipitation (CMAP) for every station, with CMAP < 800mm (green) and CMAP>800mm (blue).

c. Rainfall season delineation method

Using the daily rain gauge data, rainfall seasons are defined based on the rainfall climatology using a localised method, where each gauge station is considered independently. Here we applied the methodology from Dunning et al. (2016) to delineate the rainfall seasons for each gauging location by calculating the DOY (day of year) of season onset and cessation. This involves finding climatological rainfall anomalies from each DOY to evaluate when rainfall is consistently above the daily mean. First, we calculated the climatological mean daily rainfall (P) and standard deviation (std) for each day (i) of the calendar year at a station, and then computed the mean daily rainfall over the whole dataset for that station ($\bar{P}$). Secondly, we used these values to compute the daily anomaly (DA) as:

$$DA = \frac{P_i - \bar{P}}{std}$$

The climatological cumulative daily rainfall anomaly (CA) was then calculated using the following equation:

$$CA(d) = \sum_{i=1\ Jan}^{d} \frac{P_i - \bar{P}}{std}$$

CA was smoothed using a 60-day running mean to allow for enough rainfall memory to capture all the seasonal rainfall while accommodating variations in season length for two dominant seasons in the HAD (bimodal regime) represented by two distinct rainfall peaks within the year (Figure 2). Using fewer than 60 days (e.g. 45 or 30) resulted in more inflection points, manifesting as false-positive mini rainfall seasons which clearly did not correspond to the onset or cessation of a rainfall season when viewed in conjunction with the rainfall anomaly. A long period of smoothing is required due to the intermittency of rainfall in this region. However, this method still resulted in detection of several additional short (and dubious) ‘seasons’, based on small increases in the rolling anomaly curve. Therefore, we set a threshold on what is considered a rainfall season, selecting a value of 15 days where ‘seasons’ at or below this length are likely to be erroneous.

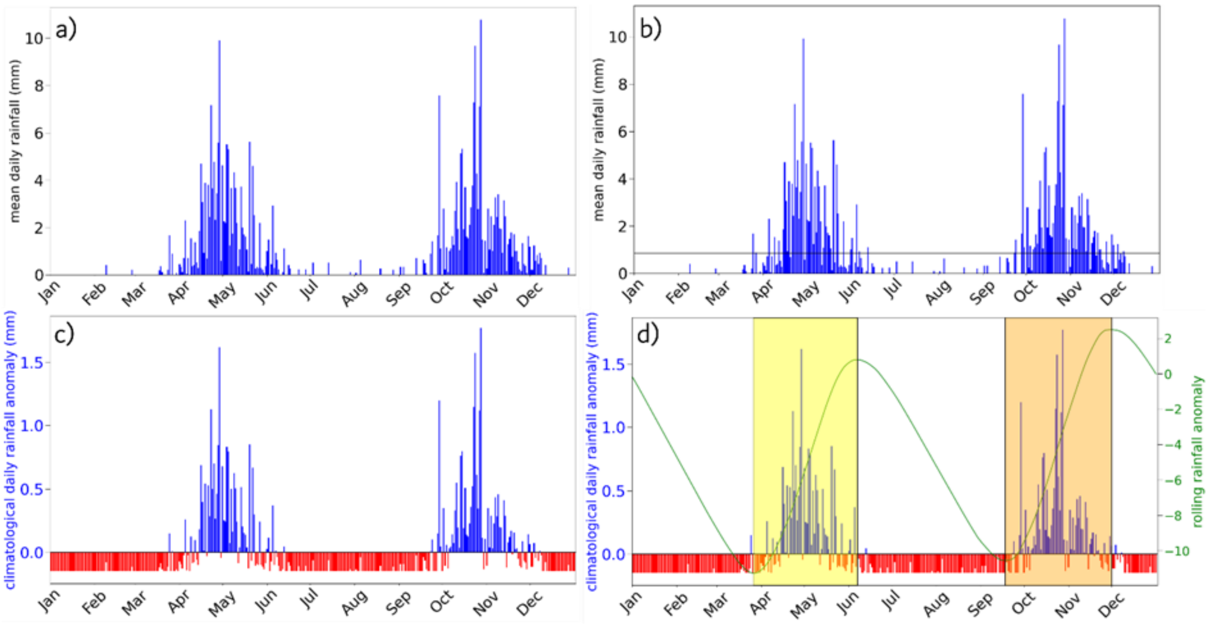

Fig. 2. Visualisation of the steps required to find season onset and cessation, shown for the example station Belet Weyne in southern Somalia. a) shows the climatological mean daily rainfall for each day of the calendar year. b) adds the daily climatological mean rainfall over all days (P) overlaid as a horizontal line. c) utilises the horizontal line in b) to find the climatological daily rainfall anomaly, where the red bars indicate days of below average rainfall, and blue bars indicate days of above average rainfall. d) utilises the climatological anomaly values from c) to find the centred, 60-day rolling daily rainfall anomaly shown in green. The timing of the LR season and SR season are shown by the yellow box and the orange box, respectively.

Figure 2 illustrates how this method generates rainfall anomalies for the Belet Weyne station, located in southern Somalia, and how this leads to delineation of rainfall seasons. The rainfall season onset is defined as the shift to a monotonically increasing value of the rolling anomaly (green line), and the cessation is defined as the shift to a monotonically decreasing value of this rolling anomaly. The resulting season is shown by the coloured boxes (Figure 2d). Belet Weyne has a distinctly bimodal regime, characterised by two rainfall seasons with 2 minimum and 2 maximum values on the rolling anomaly curve, and there is a visible gap between these seasons, indicated by the ~ 3-month period of rainfall below the yearly average shown by the red bars. Applying this method shows that for this station the LR season onset is the 27th of March and cessation is the 7th of June, and the SR season onset is the 17th of September, and the cessation is the 1st of December.

Some stations have a unimodal rainfall regime, exihibiting only one minimum and one maximum value of the rolling anomaly. These 2 stations, Gebiley and Hargeisa, correspond to the labeled numbers 4 and 5 on Figure 1a. Given that they are unimodal, we have left them out of the seasonal rainfall analysis of the LR and SR seasonsthat follow. However, unimodal stations are still discussed in terms of rainfall regime within the HAD.

d. Calculation of rainfall metrics

Before we explain the seasonal rainfall metrics, we will address the mean annual total - an annual rainfall metric. We use mean annual total as climatological metric for determining which stations should be included in the analysis of dryland rainfall. First, we calculated CMAP (figure 1) as the average annual total rainfall at each station, which was used to constrain the drylands region from which all stations are included. Later, we will view a similar metric – mean annual total. In a sense, CMAP is the same as the mean annual total since they are both calculated in the same way; the average amount of rainfall delivered each year at each station. For CMAP, this is calculated over all stations, but the mean annual total is only over dryland stations.

We subsequently used the climatological characterisations of the rainfall seasons at each location to develop a spatial analysis of differences in rainfall timings, totals, and extremes. The rainfall season onset and cessation dates were calculated in Python 3 by the method described above, resulting in onset and cessation DOY (day of year), i.e. from 1 to 365. We then used these DOYs of onset and cessation – LR season onset (LRO), LR season cessation (LRC), SR season onset (SRO), and SR season cessation (SRC) - to calculate seasonal rainfall metrics for each station. These seasonal rainfall metrics will permit us to view the spatial variability in different representations of rainfall, and how they differ between the LR and SR seasons. The season length (LR length, SR length) is computed as the cessation DOY minus the onset DOY. Mean seasonal rainfall total (mean LR total, mean SR total) is calculated as the average amount of rainfall delivery within all the LR and SRseasons at each station. The interannual variability in seasonal total (LR seasonal total stdev, SR seasonal total stdev) is calculated by the standard deviation in seasonal totals. The mean seasonal rain-days (Mean LR rain-days, Mean SR rain-days) was determined by calculating the number of days within the season that recorded an amount of rainfall 1mm or greater. This is so we can understand how many days in the rainfall season record rainfall. Seasonal consecutive dry days (LR mean max CDD, SR mean max CDD) were calculated based on the longest period of days within each LR and SR season where no rainfall was recorded, averaged over all years for each station. This metric is to inform us what the maximum length of a dry period within the rainfall season can be. The extreme rainfall metric was explored by finding the mean (over all years) sum of rainfall on days that received rainfall over the 95th percentile value (LR sum over 95th perc, SR sum over 95th perc), based on all rain-days. This metric represents how much rainfall can be accumulated on the most extreme days in the rainfall record. We also use the locally defined rainfall seasons to compare them with MAM and OND, by investigating if the local seasons capture more extremes than the MAM and OND seasons.

We also present rainfall metrics as ratios to normalise values for each station and to compare between seasons. Here, we can get more information out of the calculated metrics. The season length and mean seasonal total of each season are comapred, to view the spatial variability in which season is longer and which season recieves more rainfall. We can use these results to understand the extent to which this decline in the 'long rains' is captured climatologically. The rain-days and CDD of each season are compared against the season length, to view what proportion of days in the season deliver rainfall, and the highest proportion of the season we can expect to be composed of consistently dry conditions. The extreme rainfall metric is compared against mean seasonal total to understand what proportion of the mean seasonal total can be received as a rainfall sum of the most extreme days within the season over the historic record. We computed: 1) season length ratio (LR length/SR length); 2) seasonal rainfall total ratio (Mean LR total/Mean SR total); 3) seasonal rain-days ratio (Mean LR rain-days/LR length, Mean SR rain-days/SR length); 4) the seasonal consecutive dry days (CDD) ratio (LR mean max CDD/LR length, SR mean max CDD/SR length) 5) seasonal cumulative rainfall on extreme days ratio (LR sum over 95th perc/mean LR total, SR sum over 95th perc/mean SR total).

We spatially interpolated between the point values of these rainfall metrics over the whole study region using ordinary kriging in python with the pykridge module. Here, we used default parameters and a linear model, based on a default number of 6 averaging bins, where semi-variance at smaller lags are not weighted. The range, sill, and nugget of the variogram are calculated separately for each rainfall metric. The nugget is the value of the variogram at a lag of 0 (the y intercept), The range is the distance (x axis value) where the variogram model begins to flatten, the sill is the corresponding y axis value to the range. Ordinary kriging was used to produce spatially interpolated maps depicting the spatial variability of rainfall metrics. These spatially interpolated maps smooth data at gauge stations. The raw rainfall metric values are available in Supplemental Material Table 2. Violin plots were also constructed to statistically compare the distribution in raw values of rainfall metrics at all gauge stations in each season. Violin plots show the frequency of the data in their width, revealing additional information about the data in comparison to boxplots. The range of values shown in the violin plots are limited to the range of the raw values. More information on rainfall metric statistics are available in Supplemental Material Table 2.

3. Results

Our results are split into 5 sections: seasonal timings, rainfall season regimes, rainfall totals, rain-days and consecutive dry days, and extreme rainfall. The statistics outlined in the previous section will now be analysed.

a. Seasonal timings

Figure 3 shows the spatial variability of seasonal rainfall timings (season onset and cessation) within the HAD. For most of the extent of the HAD for the LR season, there is a southwest to northeast gradient in seasonal rainfall timing, with earlier timings in the southwest and later timings in the northeast (Figure 3a and 3b). The southern Somali coast is a marked exception to this pattern, with LR season cessation dates occurring much later here relative to inland. The raw value of cessation date at Jamame (marked with the number 3 in figure 1a) is 16th August. No such spatial gradient exists for the SR season, but the season is very early in north western Somalia and slightly late in southern Kenya compared to the OND definitions (Figure 3c and 3d).

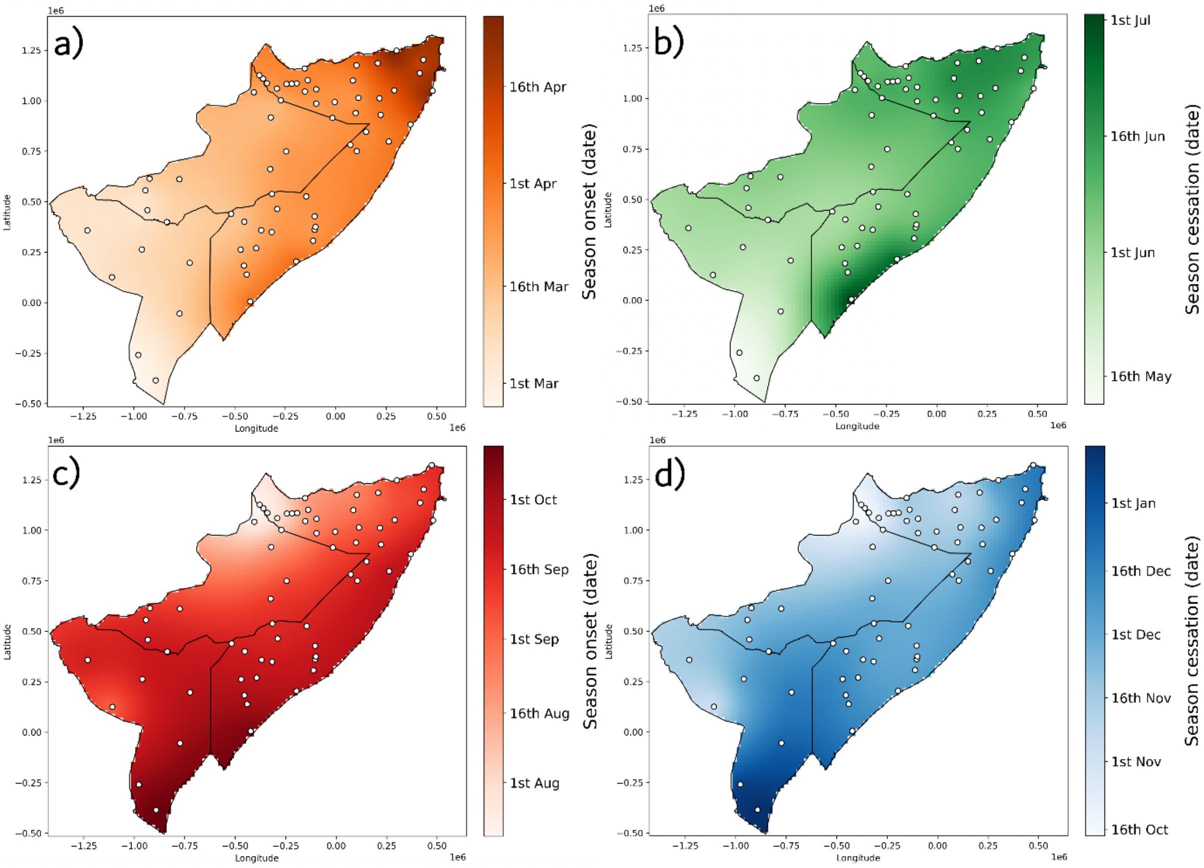

Fig. 3. Maps of spatial variability of seasonal rainfall timing. a) LR season onset, b) LR season cessation, c) SR season onset, d) SR season cessation

Figure 4 shows the rainy season calendar for the onset and cessation of each season. The LR season timing distributions have thin upper tails, representing a few stations with exceptionally late onset and cessation dates. The distributions of SR season timings are relatively narrow for earlier dates, suggesting that some stations have early starts and endings, but most are later. The interquartile range (IQR) of each seasonal onset and cessation range are: LR season onset: 13 days, LR season cessation: 15 days, SR season onset: 27 days, SR season cessation: 30 days. Note that the IQR values for the SR season for both onset and cessation are approximately double that of the LR season values, suggesting much greater spatial variability in seasonal timings for the second rainfall season of the calendar year.

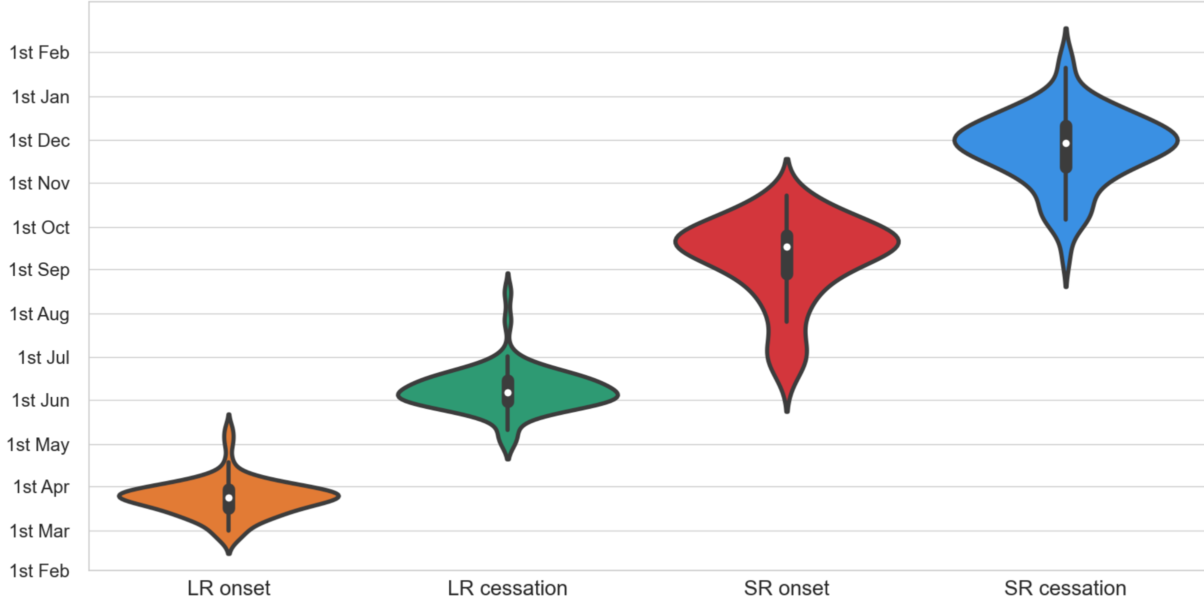

Fig. 4. Violin plots showing the rainy season calendar of seasonal rainfall timings and their spatial variability. LR season onset in orange, LR season cessation in green, SR season onset in red, SR season cessation in blue. The median dates are shown by the white dots.

Figure 5 shows the spatial variability in the length of the LR season and SR season (Fig 5a, 5b, and 5c). Figure 5c shows the frequency distribution in the length of both rainfall seasons. The thin tails here suggest that there are some stations with exceptionally short seasons in either the LR season or SR season, and that there are stations with exceptionally long seasons in the LR season. The median season lengths are 74 days and 77 days for the LR season and SR season respectively, shown by the white dots. Despite the fact that Figure 5c shows the longest rainfall seasons are observed in the LR season for the raw values, Figures 5a and 5b show that the longest rainfall seasons in the HAD for the spatially interpolated values are in the SR season in north western Somalia and at the tip of the horn in Northern Somalia, while the shortest seasons are in the LR season at the tip of the horn in Northen Somalia. Figure 5d shows the season length ratio across the HAD, demonstrating that neither the LR season or the SR season has a consistently longer duration; there is regional variation in rainfall season duration. Areas that are white (corresponding to a ratio value of 1) indicate that the LR season and SR season are roughly the same length, which comprises a surprisingly large amount of the study area. The LR season is the longer rainfall season in northwest Kenya and on the southern Somalia coast, whereas the SR season is the longer season at the coast of the horn tip in northern Somalia, and in eastern Kenya.

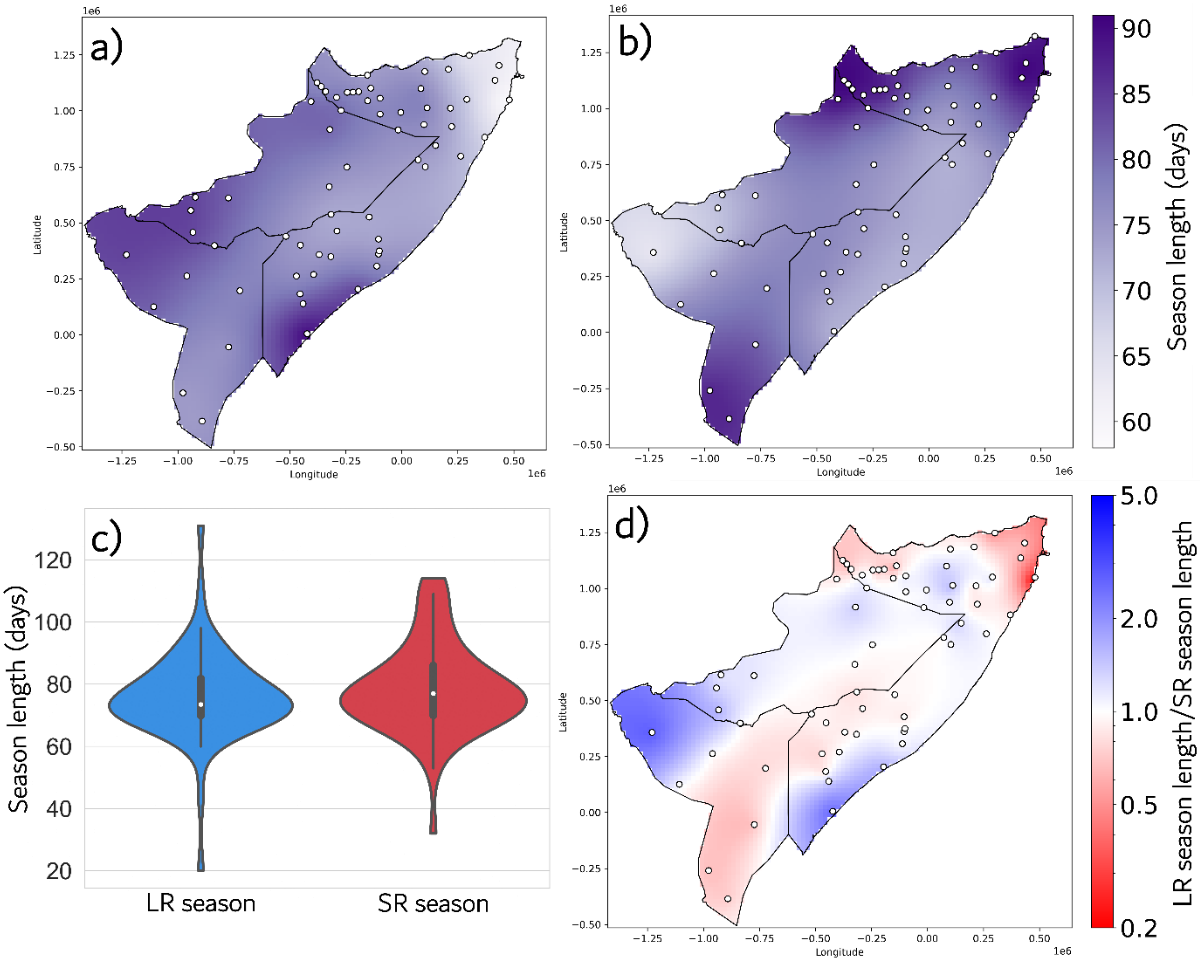

Fig. 5. Spatial variability in season length. a) spatial variability in the length of the LR season in days. b) spatial variability in the SR season in days. c) violin plots showing variability and distribution in raw values of season length d) ratio of season length, with blue indicating that the LR season is longer and red indicating that the SR season is longer.

b. Rainfall season regimes

The annual climatological rainfall anomaly at a selection of different stations reveals high variability between stations in seasonal rainfall timings and illustrates that there are different rainfall regimes across the region (Figure 6). Figure 6a shows the climatological rainfall anomaly at station 2, Wajir, in northeast Kenya (these station numbers correspond to location of labelled stations in figure 1a). This station has a distinctly bimodal regime with a rainfall season timing close to MAM and OND. This is the most common regime throughout the HAD region. Figure 6b shows the climatological rainfall anomaly at station 3, Jamame, located on the southern Somali coast. This station presents with an LR season which extends far into the summer, and a brief SR season. Figure 6c shows the climatological rainfall anomaly at Gebiley in northwestern Somalia, which – despite there being two annual rainfall peaks - presents a unimodal regime, where the method only distinguishes one minimum and one maximum value in the daily anomaly curve. This is because there is no extended period of negative rainfall anomaly between the two rainfall peaks, and the rolling anomaly curve is smoothed over a long period of time. Figure 6d shows the climatological rainfall anomaly at station 6, Callula located on the coast at the very tip of the horn in northern Somalia. It has a SR season, but no LR season. There is a very small amount of rainfall recorded around the time where the LR season would be expected, but not enough for a rainfall season to be detected using our methodology.

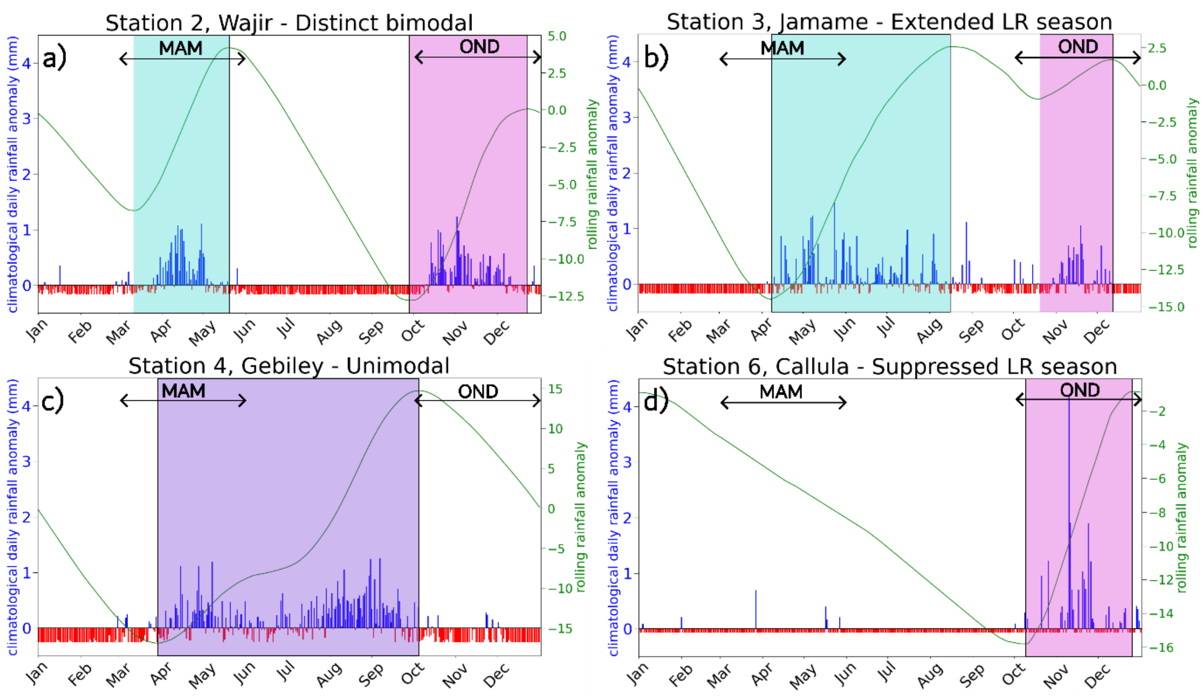

Fig. 6. Climatological rainfall anomaly at a selection of gauge stations throughout the HAD to illustrate contrasting rainfall regimes. Daily climatological rainfall anomaly (blue/red) and 60-day rolling anomaly of climatological annual rainfall (green). Black arrows indicate timings of MAM and OND. Blue, pink, and purple boxes indicate timings of local LR season, SR season and summer unimodal rainfall seasons respectively. a) distinctly bimodal regime, b) extended LR season regime, c) unimodal regime, d) supressed LR season regime. All these stations are labelled in figure 1a.

c. Rainfall Totals

Here, mean annual rainfall totals are explored spatially. Figure 7 shows there is a general gradient in rainfall within the HAD, wetter in the southwest and drier in the northeast, with a few exceptions. Climatologically, the wettest region of the study area is southern Ethiopia, and the driest region is northeastern Somalia.

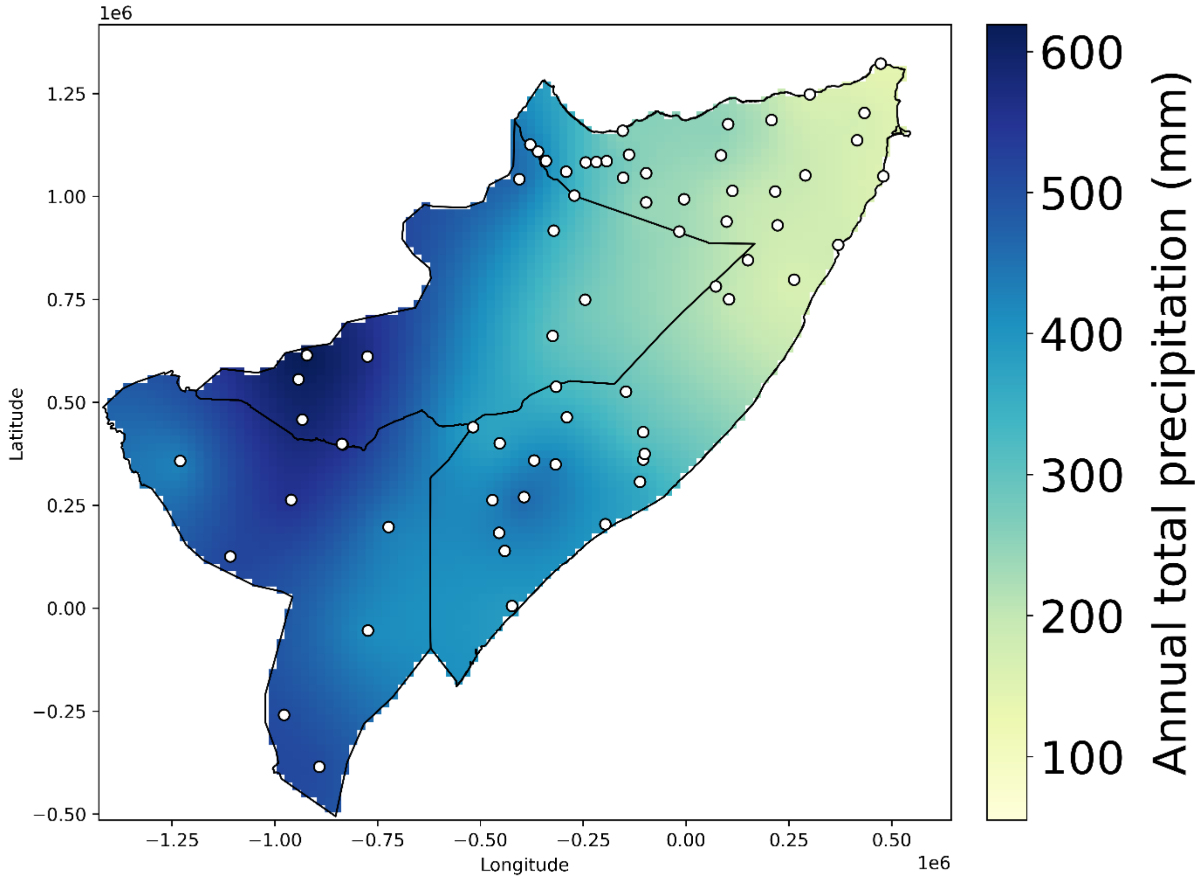

Fig. 7. Spatial variability of mean annual total precipitation for the HAD region.

Figures 8a and 8b show that northeastern Somalia is the driest region of the HAD in both seasons individually. Southern Ethiopia has the wettest LR season, and southern Kenya has the wettest SR season. The distributions shown in Figure 8c have comparable shapes and medians of 137 mm and 129 mm for the LR season and SR season respectively. Figure 8d shows the seasonal rainfall total ratio. There are similarities between Figures 8d and 5d, showing that the regions with longer seasons have correspondingly higher rainfall totals in those seasons, as one might expect. Again, as in Figure 5d, areas shown in white in Figure 8d which correspond to a ratio value of 1 indicate that the LR season and SR season both deliver a similar amount of rainfall.

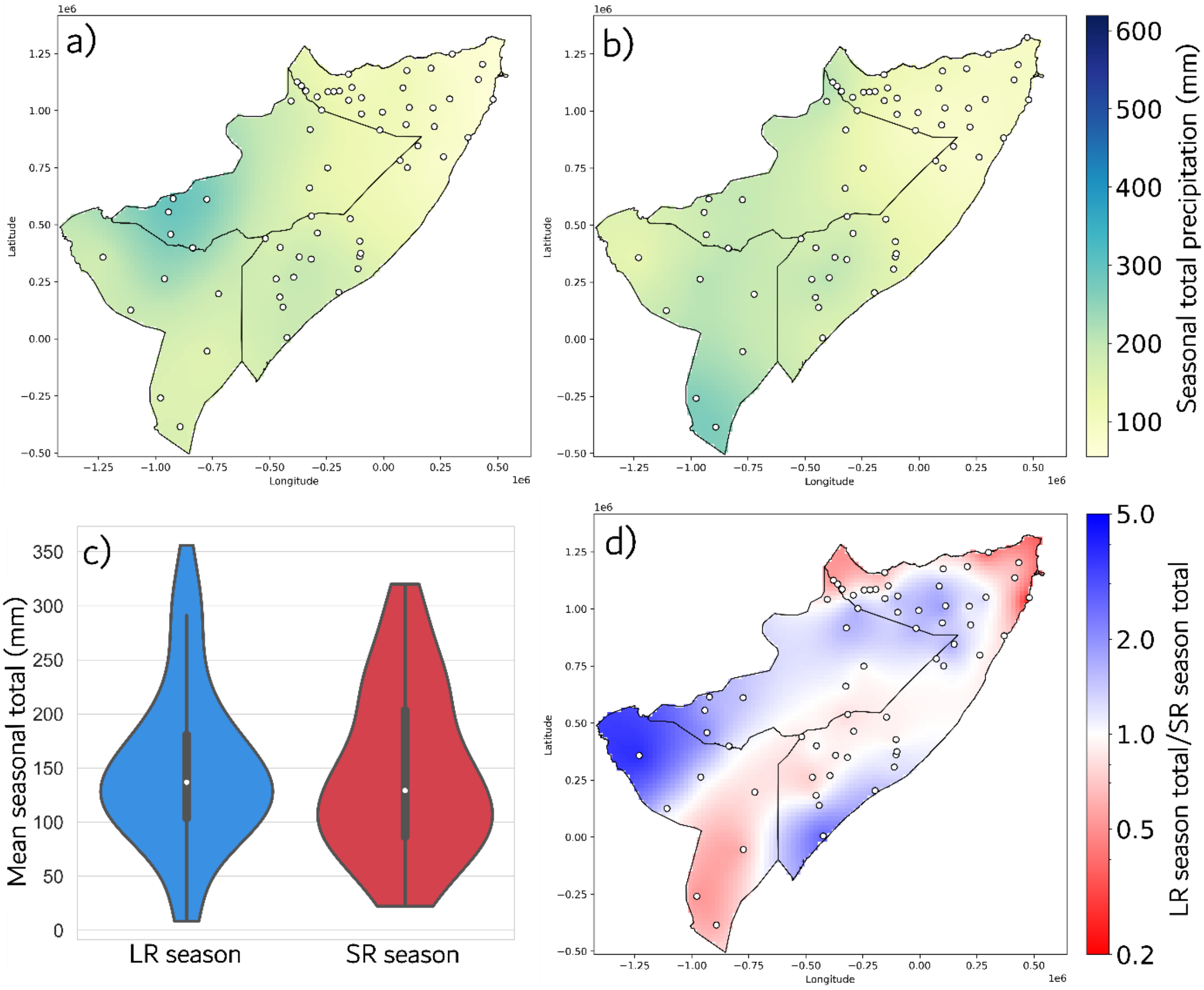

Fig. 8. Spatial variability in mean seasonal rainfall total. a) mean LR season rainfall total, b) mean SR season rainfall total, (a and b both have the same colour scale as figure 7), c) violin plots showing variability and distribution in mean seasonal rainfall total, d) ratio of mean seasonal total, with blue regions showing more rain in the LR season and red regions showing more rain in the SR season.

Figures 9a and 9b show the spatial variability of the interannual variability in seasonal total for the LR season and the SR season, respectively. The SR season displays higher interannual variability than the LR season. Eastern Kenya and southern Somalia have the highest interannual variability in mean seasonal total in the SR season. Typically, there is higher interannual variability in seasonal total in the southern HAD relative to the north. Figures 9c and 9d show the correlation between the number of rain-days and the mean seasonal total. In the LR season, most stations are clustered together, and rain is received on a relatively small number of days, resulting in low seasonal rainfall totals (Figure 9c), whereas in the SR season, there is a more even spread in the data for the number of rain-days (Figure 9d). The correlations and corresponding p values both show a strong relationship between seasonal rainfall total and seasonal rain-days in both seasons. Both SR season Figures 9b and 9d show higher spatial and interannual variability in seasonal total relative to the LR season, with b highlighting strong differences between the north (low) and south (high).

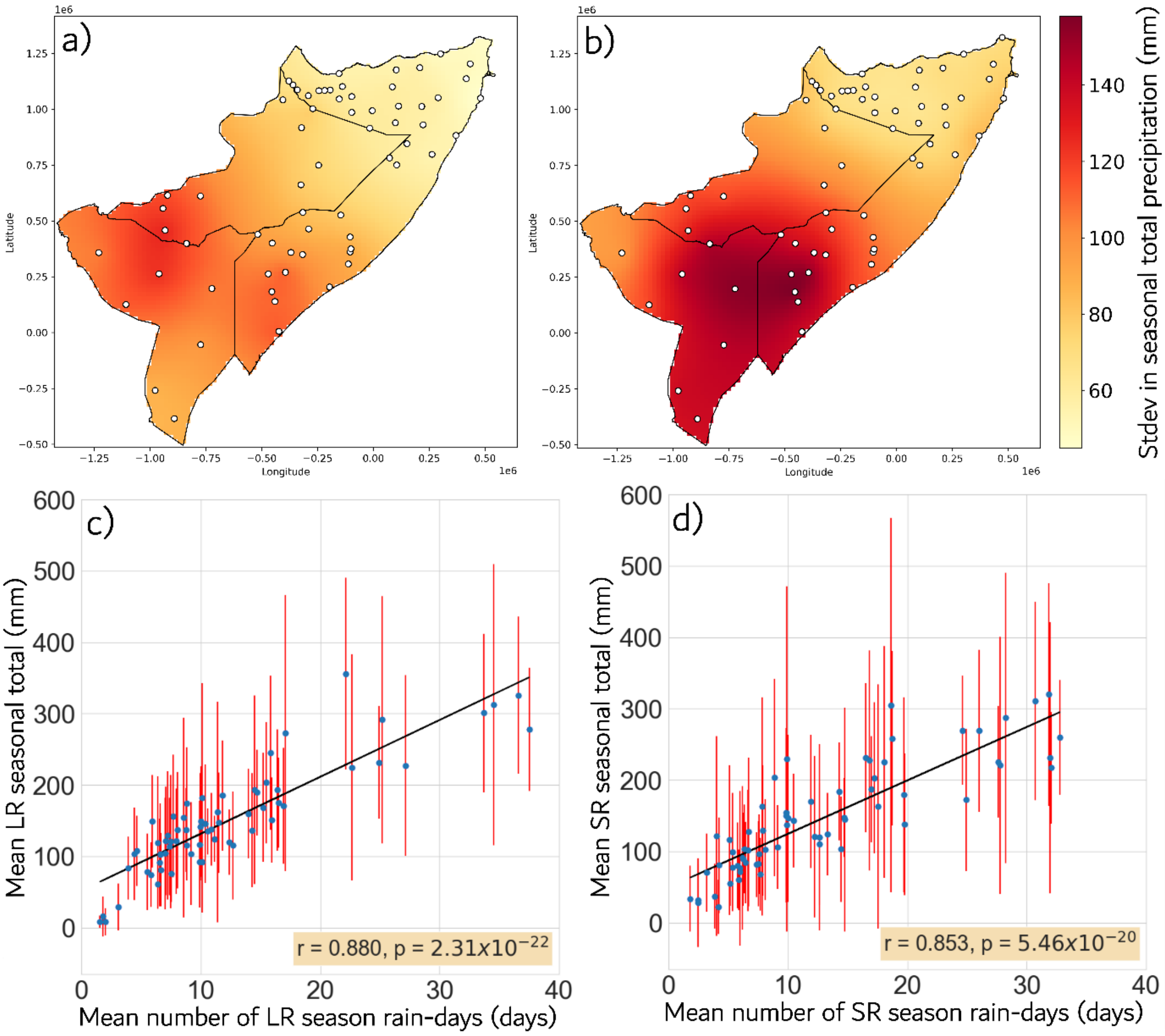

Fig. 9. Spatial variability of interannual variability in seasonal total rainfall value for the LR season (a) and the SR season (b). Correlations and line of best fit plots showing mean number of seasonal rain-days at each station (x axis) against mean seasonal rainfall total (y axis) shown by blue points, and corresponding standard deviation (interannual variability) shown in red for the LR season (c) and the SR season (d) respectively.

d. Rain-days and consecutive dry days

Figure 10 shows that the region with the most seasonal rain-days relative to season duration is southern Ethiopia, which has more rain-days in the SR season relative to the LR season. Equally, the region with the fewest rain-days in both seasons is northern Somalia, with proportionally more rains days in the LR season. In general, rainfall delivery does not exceed 30% of days in the rainfall season. In northern Somalia - the driest region of the HAD – rainfall is delivered on <10% of days within the SR season. The median ratio of rainy days within the two seasons is ~13%, which corresponds to ~10 days of rain in each season (Figure 10c).

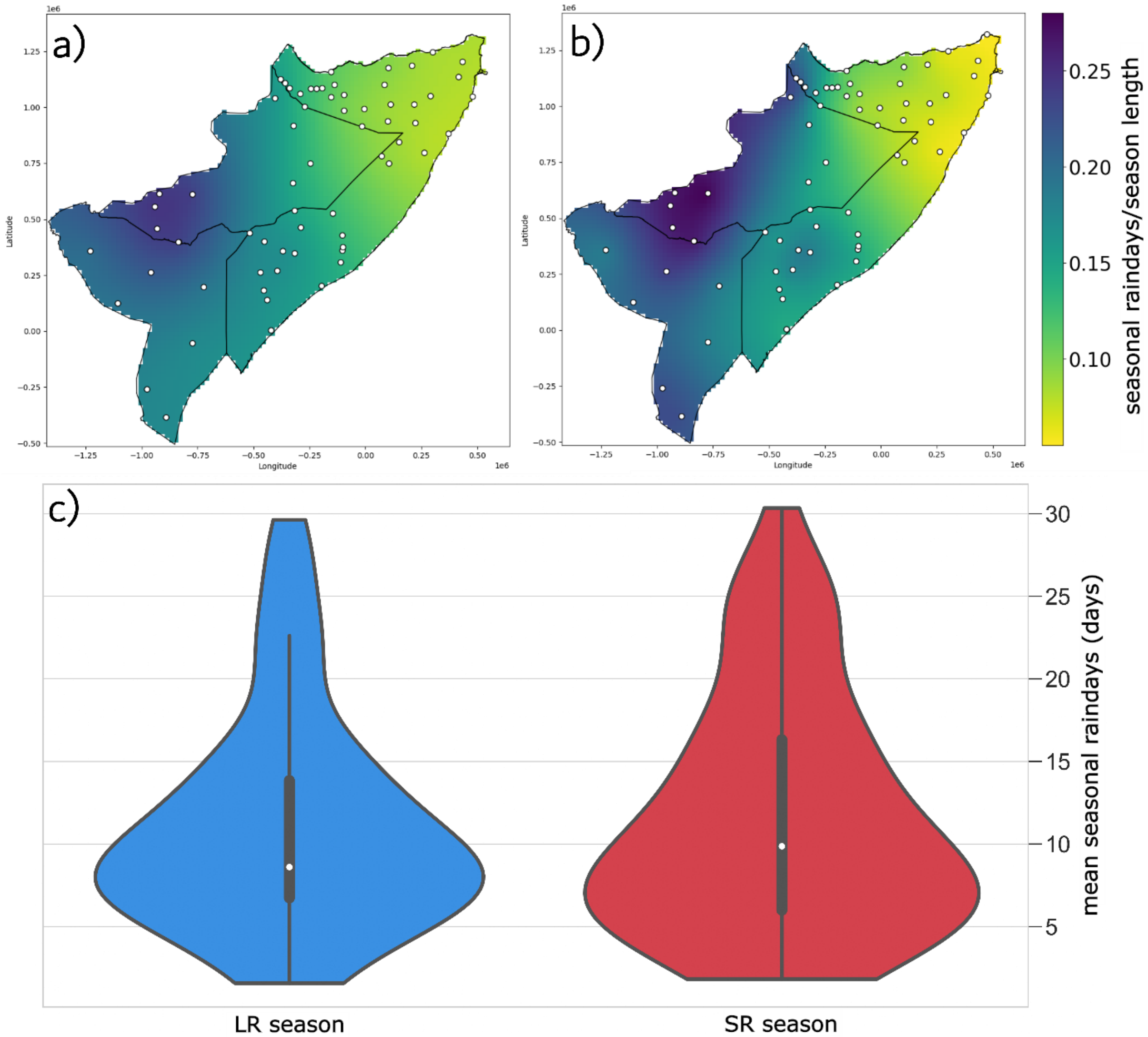

Fig. 10. Spatial variability in number of mean seasonal rain-days as a proportion of season length for the a) LR season b) SR season, and c) violin plots showing the variability and distribution in the raw values of number of seasonal rain-days.

During the LR season in the driest region (northern Somalia), some locations have recorded consecutive dry periods spanning more than 70% of the season length (Figure 11). The median values of the seasonal consecuitve dry days (CDD) ratios are 0.36 for both the LR season and SR season. In other words, it is typical for any LR or SR season to contain a dry period which takes up around one third of the season duration. These long dry periods could also be due to a delayed onset or early cessation of the rainfall season, suggesting a high interannual variability of seasonal rainfall timings (onset and cessation). The violin for the SR season in Figure 11c has a long tail, suggesting that some of the maximum raw values detected for consecutive dry conditions made up a large proportion of the season length – up to about 2 months. This would be considered a 'failed season'(Funk et al. 2023; MacLeod 2018).

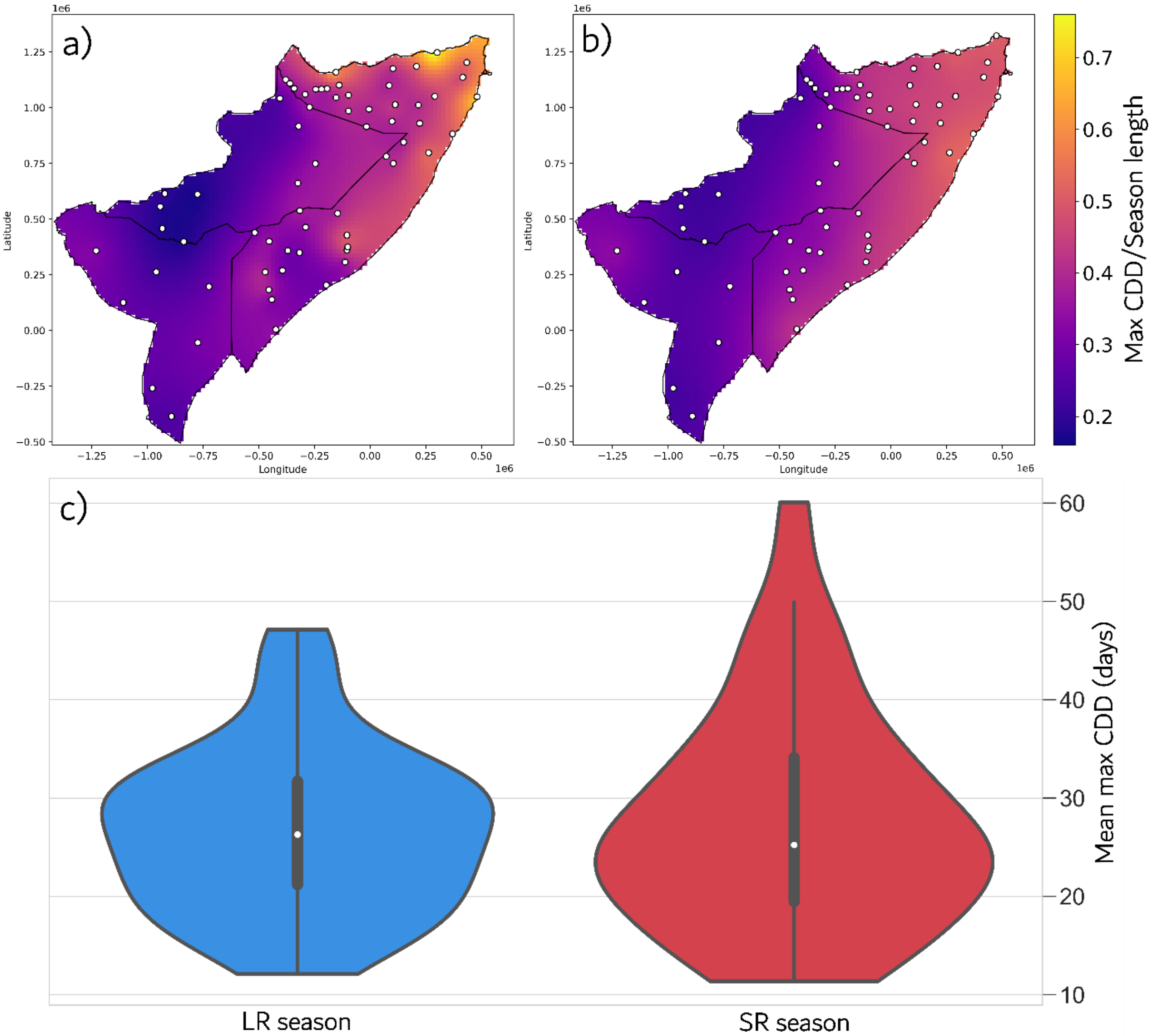

Fig. 11. Spatial variability in mean maximum number of consecutive dry days (mean max CDD) as proportion of season length for a) the LR season b) the SR season, and c) violin plots of variability and distribution in raw values of mean max consecutive dry days.

e. Extreme rainfall

In Figures 12a and 12b, values above 1 (shown in green) indicate that the mean cumulative total rainfall on rainfall days over the 95th percentile for each locally defined season across the historical record is higher than the mean seasonal total. For the LR season, this green region of extreme rainfall lies along the northern Somalia coast, and in northern Somalia for the SR season. Northwestern Kenya is also green for the SR season, indicating a local hotspot of extreme rainfall within this season. The largest seasonal cumulative extreme days value shown is around 2 during the LR season, indicating that (on average), on the northern coast of Somalia, twice the amount of rainfall was recorded on the most extreme days from the historical record, relative to the mean seasonal total. Northern Somalia is exceptionally dry, receiving mean seasonal totals <100mm, but receiving twice this annual total in one day would still be an extreme amount of rain. The lowest values of the seasonal mean cumulative extreme days ratio are in southern Ethiopia during the LR season, which is also the region with the highest mean seasonal total during this season (Figure 8a). Equally, the highest values observed for seasonal cumulative extreme days ratio are on the northern coast of Somalia, the region with one of the lowest mean seasonal totals for the LR season (Figure 8a). Therefore, the regions with the most extreme rainfall tend to receive the lowest seasonal total rainfall, and vice versa.

We also investigated if the locally defined rainfall seasons are better at capturing days of extreme rainfall, relative to the definitions of MAM and OND. We found the timings of the 5 most extreme rainfall days across the whole year, over all years for each station, then calculated how many of these extreme rainfall days are captured by the timings of the local rainfall seasons, and then by the MAM and OND seasons. We find that on average, MAM and OND pick up 85% of the most extreme rainfall days, whereas using the locally defined rainfall seasons for each station detects 91% of extreme rainfall days. This may be only a small improvement, but it must be noted that MAM and OND account for half the days in the year, with each season spanning 92 days whereas the locally defined seasons are shorter, with the mean LR and SR season lengths of 76 days and 79 days respectively (Figure 5c).

Therefore, the locally defined seasons are better suited for identifying the occurrence of extremes despite having a generally shorter duration.

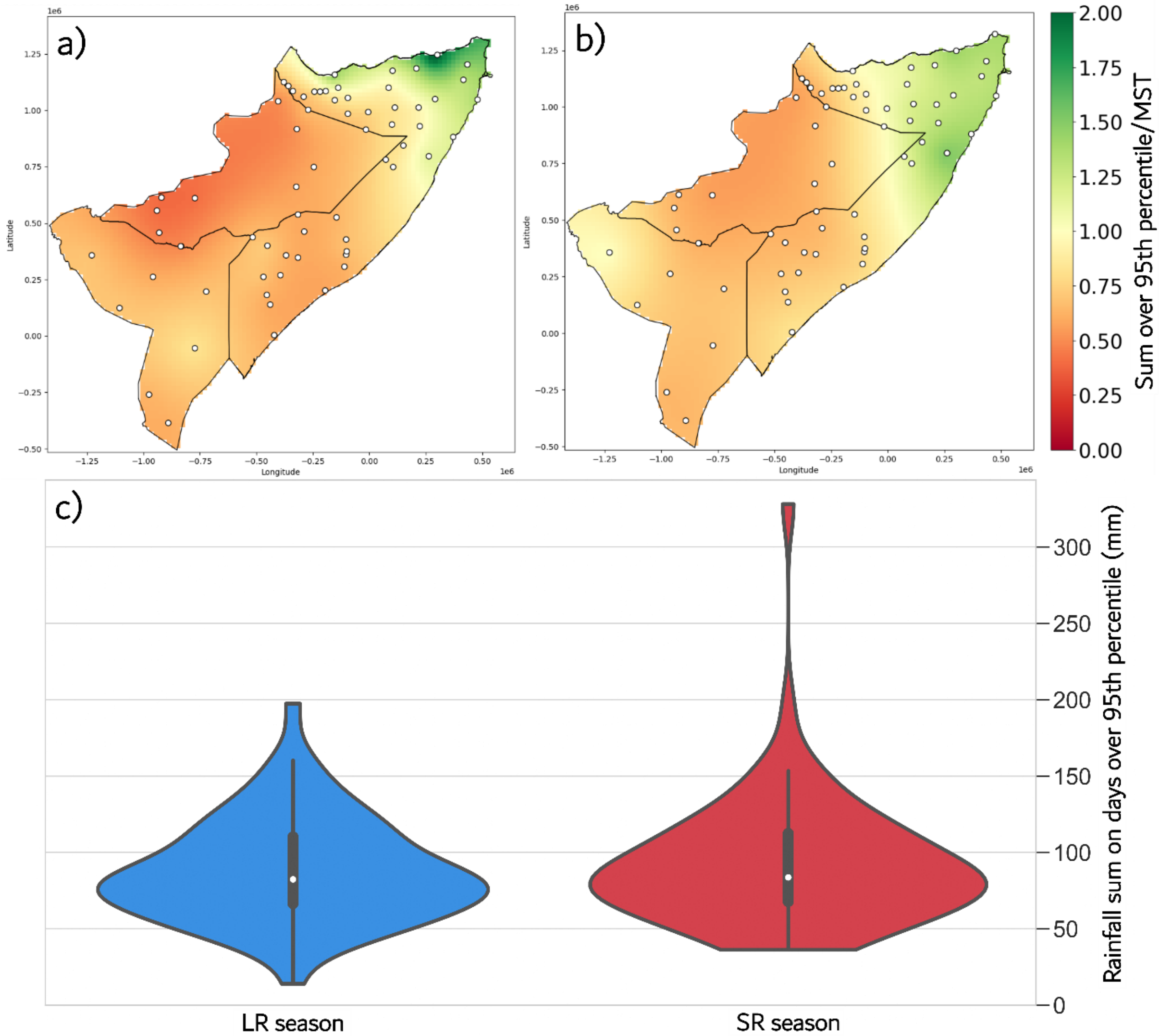

Fig. 12. Spatial variability in mean sum of rainfall days that deliver rainfall over the locally defined 95th percentile daily rainfall value as a proportion of the mean seasonal total (MST) for a) the LR season and b) the SR season and c) violin plot showing variability and distribution in the raw values of rainfall sum on days over 95th percentile at all gauges for each season.

4. Discussion

In this study, we analysed daily rain gauge data based on a method that delineates rainfall seasons in order to derive locally relevant climatological rainfall metrics. This allowed us to view the spatial variability for a range of rainfall characteristics (timings, totals, extremes) within the Horn of Africa drylands. We suggest that the locally-defined seasonal rainfall metrics presented here, based on a gauging network spanning Kenya, Somalia, and Ethiopia, provide a new window into geographical patterns of rainfall that can be used to better anticipate climate hazards within agropastoral communities who reside on the HAD, and who are reliant on the seasonal rainfall for their lives and livelihoods (Coughlan de Perez et al. 2019; Palmer et al. 2023; Pricope et al. 2013). For example, gridded remotely-sensed rainfall products that are commonly used due to a lack of in situ gauging data utilise spatial averaging, reducing the heterogeneous nature of rainfall expression and limiting the characterisation of extremes (Dinku et al. 2018; Ramos Filho et al. 2022). Local gauges present a powerful and direct picture of rainfall delivery that supports analyses of key metrics that are relevant to climatic hazards including floods and droughts. However, gridded datasets have one crucial advantage over gauge data: spatially continuous and homogeneous data coverage. Therefore, future work applying this analysis of seasonal rainfall metrics to gridded satellite data may be fruitful.

When we define the rainfall seasons locally, such that each gauge is considered independently (in contrast to most gridded analyses), strong spatial variability in rainfall timings is revealed, even after interpolation by kriging, which effectively smooths the data. The extent of this spatial variability for locally defined seasonal rainfall reveals that the terms MAM and OND are of limited value for representing the timings of the rainfall seasons across the entire HAD. Figures 3, 4 and 6 reveal how varied the timings of key rainfall seasons in this region can be. The seasonal rainfall regimes indicate that northern Somalia has a supressed LR season, and existing work shows this may be typical of the region, since timings of onset and cessation occur around the same time of year (Dunning et al. 2016; Omay et al. 2023). Also, as shown by the seasonal rainfall regimes, the southern coast of Somalia can experience a LR season that extends into July. This apparent extended rainfall season is due to the interaction between sea breeze flow, and the south-west monsoon (Ashford 1998; Camberlin and Planchon 1997). It is already known that in the Somaliland region, the cessation of the LR season is said to occur in June, and onset of the SR season is said to occur in August (see Table 1). However, at some stations these ‘seasons’ occur so close together in time that the method employed here cannot distinguish these rainfall modes from each other, so only one rainfall season is detected. The stations that (according to the method employed here) have a unimodal regime (Gebiley and Hargeisa), are in western Somaliland which lies on the boundary of the unimodal rainfall region (Dunning et al. 2016; Omay et al. 2023; Seregina et al. 2019). Therefore, whether these stations have a unimodal or bimodal regime is up to interpretation.

Our results suggest that there is spatial variability in which season delivers the most rainfall, and there are many regions where there is more rainfall in the SR season relative to the LR season (Figure 8d). This could be explained by the fact that data used in this study are from the 1990s onwards, coinciding with the decline of the 'long rains'(Hoell et al. 2017; Liebmann et al. 2017; Lyon and DeWitt 2012), which could have led to discrepancies in the relative seasonal rainfall totals compared to the historical norms which delineated the seasons. In other words, our results may be capturing the recent decline of the LR season which could also explain why these results deviate from conventional understanding of season length (Figure 5d). However, there has been recognition that the SR season delivers a larger proportion of rainfall in southeastern Kenya than the LR season (Camberlin and Wairoto 1997), an observation which aligns more closely with our results (Figure 8d).

Results of seasonal cumulative extreme days ratio (Figure 12) indicate that in northeastern Somalia, the most extreme rainfall days from the historic record accumulate to more than the mean seasonal total. Rainfall total results (Figures 7 and 8) also indicate that this is the driest region of the HAD. Receiving high rainfall amounts in a short period of time where normal conditions are extremely dry indicates this region could be more exposed to impacts of extreme rainfall such as flash flooding and landslides, leading to infrastructure damage and loss of life (Chang'a et al. 2020; Hooke 2019; Middleton and Sternberg 2013). On the other hand, extreme rainfall in drylands is also the main contributor of focussed groundwater recharge, leaving potential for groundwater usage for irrigation, if aquifers are to be used sustainably (Adloff et al. 2022; Cuthbert et al. 2019; Taylor et al. 2013).

Our method and results of local rainfall season delineation could lay the foundations for a more locally relevant rainfall season forecast that could be provided by ICPAC within the GHACOF and by national hydrometeorological services who issue early warnings about seasonal climatic hazards. For example, if rainfall forecasts were benchmarked against locally defined rainfall seasons, early warnings and advisories could be developed that comport with local experiences, which could potentially build more trust between climate service providers and end users of climate information (Kadi et al. 2011; Leavy 2016; Rigby et al. 2022).

5. Conclusion

Despite the uneven regional distribution of rain gauges, the findings of this study provide a new perspective on the rainfall seasons within the HAD, which consider the climatology of local rainfall characteristics and their spatial variability. Our results have shown that MAM and OND – despite being useful rainfall timings for the HAD in a general sense – fall short when applied the local scale. Extreme rainfall results indicate that the rainfall sum on the most extreme days throughout the historical record can be up to twice the value of the mean seasonal total. Our analysis comparing the length and rainfall totals of the rainfall seasons show that our data may hold information on the recent drying of the LR season, and that it may no longer be appropriate to continue to think of the LR season as the 'main rainfall season'. Insights into localised rainfall seasons may provide more improved and relevant decision-support tools and aid in the identification and predictability of climate hazards for the rural communities that live across the HAD who are reliant on this rainfall for agriculture and pastoralism. By accounting for local definitions of seasonality, climate service providers such as ICPAC through the GHACOF can ensure that outputs such as seasonal forecasts align with the local experience, and so increase their relevance and potential uptake.

6. Future work

The results in Figures 5d and 8d suggest equal ratios in season length and rainfall total between seasons in areas that are sparsely gauged. It may be beneficial to perform a comparison using a gridded satellite rainfall product to check for corroboration with the kriging. Specifically, it would be useful to check if these areas with a ratio value close to 1 present a similar result when satellite rainfall data is used. In general, it would be beneficial to compare any of these metrics with a satellite rainfall product to validate and test the utility of these gauge data, also observing how results differ in areas that are more densely gauged.

Acknowledgements

We acknowledge PhD studentship funding from both Cardiff University College of Physical Sciences and Engineering, and DOWN2EARTH, an EU Horizon 2020 Project funded under grant agreement No 869550. We also thank the Food and Agriculture Organisation of the United Nations - Somalia Water and Land Information Management (FAO-SWALIM), Kenya Meteorological Department (KMD), and Ethiopian Meteorological Institute (EMI) for providing the rain gauge data for this research.

Data availability statement

The Somalia rain gauge data can be accessed from https://climseries.faoswalim.org/station/map/mrs/. The rain gauge data for Kenya and Ethiopia can be accessed upon request from Kenya Meteorological Department (KMD), and

Ethiopian Meteorological Institute (EMI) respectively. The contact URLs for these organisations are as follows: KMD: https://meteo.go.ke/ EMI: http://www.ethiomet.gov.et/

REFERENCES

Abdulkadir, G., 2017: Assessment of drought recurrence in Somaliland: Causes, impacts and mitigations. *Journal Climatology Weather. Forecasting*, **5**.

Abebe, M., 2006: The onset, cessation and dry spells of the small rainy season (Belg) of Ethiopia, 41 pp.

Adloff, M., and Coauthors, 2022: Sustained water storage in Horn of Africa drylands dominated by seasonal rainfall extremes. *Geophysical Research Letter*, **49**.

Ageet, S., A. H. Fink, M. Maranan, J. E. Diem, J. Hartter, A. Ssali, and P. Ayabagabo, 2022: Validation of Satellite Rainfall Estimates over Equatorial East Africa. *Journal of Hydrometeorology*, **23,** 129–151.

Amwata, D. A., D. M. Nyariki, and N. R. K. Musimba, 2016: Factors Influencing Pastoral and Agropastoral Household Vulnerability to Food Insecurity in the Drylands of Kenya: A Case Study of Kajiado and Makueni Counties. *Journal of International Development*, **28**.

Asfaw, D. T., and Coauthors, 2022: stoPET v1. 0: A stochastic potential evapotranspiration generator for simulation of climate change impacts. *Geoscientific Model Development Discussions*, **16,** 21.

Ashford, O. M., 1998: The climate of Somalia. *Birds of Somalia*, Pica Press., 66-68.

Bekele-Biratu, E., W. M. Thiaw, and D. Korecha, 2018: Sub-seasonal variability of the Belg rains in Ethiopia. *International Journal of Climatology*, **38,** 2940-2953.

Bekele, G., and T. Abera, 2008: Livelihoods-based Drought Response in Ethiopia: Impact Assessment of Livestock Feed Supplementation, 20 pp.

Birhanu, Z., A. Ambelu, N. Berhanu, A. Tesfaye, and K. Woldemichael, 2017: Understanding resilience dimensions and adaptive strategies to the impact of recurrent droughts in Borana Zone, Oromia Region, Ethiopia: A grounded theory approach. *International journal of environmental research and public health*, **14**.

Camberlin, P., and J. G. Wairoto, 1997: Intraseasonal wind anomalies related to wet and dry spells during the “long” and “short” rainy seasons in Kenya. *Theoretical and applied climatology*, **58,** 57-69.

Camberlin, P., and O. Planchon, 1997: Coastal precipitation regimes in Kenya. *Geografiska Annaler: Series A, Physical Geography*, **79,** 109-119.

Camberlin, P., and N. Philippon, 2002: The East African March–May rainy season: Associated atmospheric dynamics and predictability over the 1968–97 period. *Journal of climate*, **15,** 1002-1019.

Camberlin, P., and R. E. Okoola, 2003: The onset and cessation of the "long rains" in eastern Africa and their interannual variability. *Theoretical and Applied Climatology*, **75,** 43-54.

Cattani, E., A. Merino, J. A. Guijarro, and V. Levizzani, 2018: East Africa rainfall trends and variability 1983–2015 using three long-term satellite products. *Remote Sensing*, **10**.

Cavalcante, R. B. L., D. B. da Silva Ferreira, P. R. M. Pontes, R. G. Tedeschi, C. P. W. da Costa, and E. B. de Souza, 2020: Evaluation of extreme rainfall indices from CHIRPS precipitation estimates over the Brazilian Amazonia. *Atmospheric Research*, **238**.

Chang'a, L. B., and Coauthors, 2020: Understanding the evolution and socio-economic impacts of the extreme rainfall events in March-May 2017 to 2020 in East Africa. *Atmospheric and Climate Sciences*, **10**.

Conway, D., E. Allison, R. Felstead, and M. Goulden, 2005: Rainfall variability in East Africa: implications for natural resources management and livelihoods. *Philosophical Transactions of the Royal Society A: Mathematical, Physical and Engineering Sciences*, **363,** 49-54.

Coughlan de Perez, E., M. van Aalst, R. Choularton, B. van den Hurk, S. Mason, H. Nissan, and S. Schwager, 2019: From rain to famine: assessing the utility of rainfall observations and seasonal forecasts to anticipate food insecurity in East Africa. *Food security*, **11,** 57-68.

Cuthbert, M. O., and Coauthors, 2019: Observed controls on resilience of groundwater to climate variability in sub-Saharan Africa. *Nature*, **572**.

Degefu, M. A., Y. Tadesse, and W. Bewket, 2021: Observed changes in rainfall amount and extreme events in southeastern Ethiopia, 1955–2015. *Theoretical and Applied Climatology*, **144,** 967-983.

Dinku, T., C. Funk, P. Peterson, R. Maidment, T. Tadesse, H. Gadain, and P. Ceccato, 2018: Validation of the CHIRPS satellite rainfall estimates over eastern Africa. *Quarterly Journal of the Royal Meteorological Society*, **144,** 292-312.

Dunning, C. M., E. C. L. Black, and R. P. Allan, 2016: The onset and cessation of seasonal rainfall over Africa. *Journal of Geophysical Research: Atmospheres*, **121,** 11405-11424.

Funk, C., and Coauthors, 2023: Frequent but Predictable Droughts in East Africa Driven by A Walker Circulation Intensification. *Earth's Future*, **11**.

Funk, C., and Coauthors, 2019: Recognizing the Famine Early Warning Systems Network: Over 30 Years of Drought Early Warning Science Advances and Partnerships Promoting Global Food Security. *Bulletin of the American Meteorological Society*, **100,** 1011–1027.

Gamoyo, M., C. Reason, and D. Obura, 2015: Rainfall variability over the East African coast. *Theoretical and Applied Climatology*, **120,** 311-322.

Garnham, P. C. C., 1945: The role of Anopheles pharoensis Theobald in the transmission of malaria in Kenya Colony. *Annals of Tropical Medicine & Parasitology*, **39,** 63-65.

Gebrechorkos, S. H., S. Hülsmann, and C. Bernhofer, 2019: Long-term trends in rainfall and temperature using high-resolution climate datasets in East Africa. *Scientific reports*, **9,** 11376.

Harrison, L., C. Funk, and P. Peterson, 2019: Identifying changing precipitation extremes in Sub-Saharan Africa with gauge and satellite products. *Environmental Research Letters*, **14**.

Hastenrath, S., D. Polzin, and C. Mutai, 2011: Circulation mechanisms of Kenya rainfall anomalies. *Journal of Climate*, **24,** 404-412.

Hoell, A., and C. Funk, 2014: Indo-Pacific sea surface temperature influences on failed consecutive rainy seasons over eastern Africa. *Climate dynamics*, **43,** 1645-1660.

Hoell, A., M. Hoerling, J. Eischeid, X. W. Quan, and B. Liebmann, 2017: Reconciling theories for human and natural attribution of recent East Africa drying. *Journal of Climate*, **30,** 1939-1957.

Hooke, J. M., 2019: Extreme sediment fluxes in a dryland flash flood. *Scientific Report*, **9,** 1686.

Horton, R. E., 1933: The role of infiltration in the hydrologic cycle. *Transactions of the American Geophysical Union*, **14,** 446-460.

Jones, R. J., and T. R. Evans, 1961: The establishment and production of a ley. *East African Agricultural and Forestry Journal*, **27,** 85-90.

Kadi, H. A., L. N. Njau, J. Mwikya, and A. Kamga, 2011: The state of climate information services for agriculture and food security in East African countries. *CCAFS Working Paper*.

Kenworthy, J. M., 2020: How Europeans experienced and observed the climate of the Kenya highlands before the establishment of the British East African Meteorological Service in 1929 *The Royal Meteorological Society: Occasional Papers on Meteorological History*, **19**.

Leavy, J., 2016: How to get communities in east Africa to trust climate science. The Conversation

Liebmann, B., and Coauthors, 2017: Climatology and interannual variability of boreal spring wet season precipitation in the eastern Horn of Africa and implications for its recent decline. *Journal of Climate*, **30,** 3867-3886.

Lyon, B., 2014: Seasonal drought in the Greater Horn of Africa and its recent increase during the March–May long rains. *Journal of Climate*, **27,** 7953-7975.

Lyon, B., and D. G. DeWitt, 2012: A recent and abrupt decline in the East African long rains. *Geophysical Research Letters*, **39**.

Lyon, B., and N. Vigaud, 2017: Unraveling East Africa's climate paradox. *Climate extremes: Patterns and mechanisms*, S.-Y. Simon Wang, Jin-Ho Yoon, Christopher C. Funk, and R. R. Gillies, Eds., 265-281.

MacLeod, D., 2018: Seasonal predictability of onset and cessation of the east African rains. *Weather and climate extremes*, **21,** 27-35.

MacLeod, D., and Coauthors, 2023: Translating seasonal climate forecasts into water balance forecasts for decision making. *PLOS Climate*, **2**.

Mady, B., P. Lehmann, S. M. Gorelick, and D. Or, 2020: Distribution of small seasonal reservoirs in semi-arid regions and associated evaporative losses. *Environmental Research Communications*, **2**.

Magombeyi, M. S., A. E. Taigbenu, and J. Barron, 2018: Effectiveness of agricultural water management technologies on rainfed cereals crop yield and runoff in semi-arid catchment: a meta-analysis. *International Journal of Agricultural Sustainability*, **16,** 418-441.

Matanó, A., M. C. de Ruiter, J. Koehler, P. J. Ward, and A. F. Van Loon, 2022: Caught Between Extremes: Understanding Human-Water Interactions During Drought-To-Flood Events in the Horn of Africa. *Earth's Future*, **10**.

Mati, B. M., 2005: Overview of water and soil nutrient management under smallholder rain-fed agriculture in East Africa. International Water Management Institute Working Paper 105. 94.

Middleton, N. J., and T. Sternberg, 2013: Climate hazards in drylands: A review. *Earth-Science Reviews*, **126,** 48-57.

Mtewele, Z. F., X. Xu, and G. Jia, 2021: Heterogeneous trends of precipitation extremes in recent two decades over East Africa. *Journal of Meteorological Research*, **35,** 1057-1073.

Muthoni, F. K., and Coauthors, 2019: Long-term spatial-temporal trends and variability of rainfall over Eastern and Southern Africa. *Theoretical and Applied Climatology*, **137,** 1869-1882.

Nicholson, S. E., 2011: *Dryland Climatology.*

Nkunzimana, A., S. Bi, M. A. A. Alriah, T. Zhi, and N. A. D. Kur, 2020: Comparative analysis of the performance of satellite-based rainfall products over various topographical unities in central East Africa: case of Burundi. *Earth and Space Science*, **7**.

Nyakudya, I. W., and L. Stroosnijder, 2015: Conservation tillage of rainfed maize in semi-arid Zimbabwe: A review. *Soil and Tillage Research*, **145,** 184-197.

OCHA, 2023: Horn of Africa Drought Regional Humanitarian Overview & Call to Action (Revised 26 May 2023).

Ogallo, L. A., G. Ouma, and P. Omondi, 2017: Changes in rainfall and surface temperature over lower Jubba, Somalia. *Journal of Climate*, **1**.

Omay, P. O., N. J. Muthama, C. Oludhe, J. M. Kinama, G. Artan, and Z. Atheru, 2023: Changes and variability in rainfall onset, cessation, and length of rainy season in the IGAD region of Eastern Africa. *Theoretical and Applied Climatology*, **152,** 871-893.

Ongoma, V., and H. Chen, 2017: Temporal and spatial variability of temperature and precipitation over East Africa from 1951 to 2010. *Meteorology and Atmospheric Physics*, **129,** 131-144.

Onyango, O. A., 2014: Analysis of meteorological drought in north eastern province of Kenya. *Journal of Earth Science & Climatic Change*, **5**.

Palmer, P. I., and Coauthors, 2023: Drivers and impacts of Eastern African rainfall variability. *Nature Reviews Earth & Environment*, **4,** 254-270.

Pricope, N. G., G. Husak, D. Lopez-Carr, C. Funk, and J. Michaelsen, 2013: The climate-population nexus in the East African Horn: Emerging degradation trends in rangeland and pastoral livelihood zones. *Global environmental change*, **23,** 1525-1541.

Ramos Filho, G. M., V. H. R. Coelho, E. da Silva Freitas, Y. Xuan, L. Brocca, and C. das Neves Almeida, 2022: Regional-scale evaluation of 14 satellite-based precipitation products in characterising extreme events and delineating rainfall thresholds for flood hazards. *Atmospheric Research*, **276**.

Rigby, J. M., M. A. Yohannis, C. Preist, M. B. Singer, T. M. Waema, A. N. Wausi, and K. Michaelides, 2022: Climate services for the Greater Horn of Africa: interviews exploring practitioner perspectives from Kenya and beyond. *Climate and Development*, **15,** 188-200.

Samwel, J. K., 2015: Impact of climate variability and change on rain-fed farming system in selected semi-arid areas of Tanzania. Doctoral dissertation, Sokoine University of Agriculture.

Schwarzwald, K., R. Seager, M. Ting, and A. Giannini, 2023: Large-scale stability and the greater Horn of Africa long and short rains. *Journal of Climate*, **36,** 7297-7317.

Seleshi, Y., and U. Zanke, 2004: Recent changes in rainfall and rainy days in Ethiopia. *International Journal of Climatology: A Journal of the Royal Meteorological Society*, **24,** 973-983.

Seregina, L. S., A. H. Fink, R. van der Linden, N. A. Elagib, and J. G. Pinto, 2019: A new and flexible rainy season definition: Validation for the Greater Horn of Africa and application to rainfall trends. *International Journal of Climatology*, **39,** 989-1012.

Singer, M. B., and Coauthors, 2021: Hourly potential evapotranspiration at 0.1 resolution for the global land surface from 1981-present. *Scientific Data*, **8**.

Taylor, R. G., M. C. Todd, L. Kongola, L. Maurice, E. Nahozya, H. Sanga, and A. M. MacDonald, 2013: Evidence of the dependence of groundwater resources on extreme rainfall in East Africa. *Nature Climate Change*, **3,** 374-378.

Verdin, J., C. Funk, G. Senay, and R. Choularton, 2005: Climate science and famine early warning. *Philosophical Transactions of the Royal Society B: Biological Sciences*, **360,** 2155-2168.

Wainwright, C. M., J. H. Marsham, R. J. Keane, D. P. Rowell, D. L. Finney, E. Black, and R. P. Allan, 2019: 'Eastern African Paradox' rainfall decline due to shorter not less intense Long Rains. *npj Climate and Atmospheric Science*, **2**.

Way-Henthorne, J., 2022: Why CHC is Confident the 2022 March-April-May Drought in Somalia, Ethiopia, and Kenya was the Worst on Record. *Climate Hazards Center*, C. Funk, Ed.

Yang, W., R. Seager, M. A. Cane, and B. Lyon, 2015: The annual cycle of East African precipitation. *Journal of Climate*, **28,** .2385-2404.